Advances in Concrete Construction, *Vol. 10, No. 1 (2020) 35-48*
DOI: https://doi.org/10.12989/acc.2020.10.1.035

Flexural strengthening of RCC beams using FRPs and ferrocement - a comparative study

N. Ganesan*, P. Bindurani[a] and P.V. Indira[b]

Department of Civil Engineering, National Institute of Technology Calicut, Kozhikode, Kerala, 673601, India

(*Received January 23, 2020, Revised May 28, 2020, Accepted June 16, 2020*)

Abstract. This paper deals with a comparative study among three different rehabilitation techniques, namely, (i) carbon fibre reinforced polymer (CFRP), (ii) glass fibre reinforced polymer (GFRP) and (iii) ferrocement on the flexural strengthening of reinforced cement concrete (RCC) beams. As these different techniques have to be compared on a level playing field, tensile coupon tests have been carried out initially for GFRP, CFRP and ferrocement and the number of layers required in each of these composites in terms of the tensile strength. It was found that for the selected constituents of the composites, one layer of CFRP was equivalent to three layers of GFRP and five layers of wiremesh reinforcement in ferrocement. Rehabilitation of RCC beams using these equivalent laminates shows that all the three composites performed in a similar way and are comparable. The parameters selected in this study were (i) the strengthening material and (ii) the level of pre-distress induced to the beams prior to the rehabilitation. It was noticed that, as the levels of pre-distress decreases, the percentage attainment of flexural capacity and flexural stiffness of the rehabilitated beams increases for all the three selected composites used for rehabilitation. Load-deflection behavior, failure modes, energy absorption capacity, displacement ductility and curvature ductility were compared among these composites and at different distress levels for each composite. The results indicate that ferrocement showed a better performance in terms of ductility than other FRPs, and between the FRPs, GFRP exhibited a better ductility than the CFRP counterpart.

Keywords: ferrocement; CFRP; GFRP; flexural strengthening; rehabilitation

1. Introduction

Concrete structures often develop structural distress due to several reasons like overloading, construction/design deficiencies, effect of natural disasters etc. Demolition and reconstruction of the deteriorated or structurally damaged structures are not always feasible, mainly due to the constraints on infrastructure budgets and the considerations of sustainable development. A reasonable solution is the rehabilitation of such structures under distress. Various methods are available for rehabilitation like jacketing techniques, epoxy-bonded steel plates, external post-tensioning etc. FRP strengthening is one of the latest evolved technologies, which is proved to be efficient by various studies around the globe (Ganesh and Murthy 2019, Aravind *et al*. 2013, Sarker *et al*. 2011, Al-Salloum and Almusallam 2003, Bakis *et al*. 2002, Ritchie *et al*. 1991). FRP laminates that bonded externally to the structural elements by wet lay-up procedure can be effectively used for strengthening purposes. The advantages of FRP like high strength to weight ratio, minimal change in structural geometry, corrosion resistance, easy and rapid installation etc. increase the acceptance of FRP as a strengthening material; but, the possible health hazards in handling FRP materials, its high cost and susceptibility to high temperature are some concerns (Siddika *et al*. 2020, Naser *et al*. 2019, Amran *et al*. 2018). Ferrocement is another proven, economic technique for rehabilitation, which possesses many of the advantages of FRP and hardly observed any health problems (Naaman 2012). Even though a lot of studies were conducted on the strengthening aspect of either FRP (Nayak *et al*. 2018, Kabir *et al*. 2018, Wan *et al.* 2018, Wang *et al*. 2018, Sumathi and Arun 2017, Sun *et al*. 2017, Venkateswarlu and Natarajan 2015, Kim and Harries 2013, Saxena *et al.* 2008) or ferrocement (Jayasree *et al.* 2016, Ebead 2015, Khan *et al.* 2013, Masood *et al*. 2005, Nassif and Najm 2004, Al-Kubaisy and Jumaat 2000), the studies on comparison of ferrocement with FRPs on their rehabilitation potential are scarce. Hence, an attempt is made in this direction. In order to create a level playing field, since different composites with different properties have been used for strengthening the specimens, the composites have to be equivalent in terms of their tensile strength. By doing so, the equivalent number of layers of FRPs and ferrocement can be obtained. Certain comparative studies available in literature did not take this aspect into consideration (Escrig *et al.* 2017, Qeshta *et al.* 2015), and this drawback was addressed in this study by finding the equivalent laminates of the selected composites.

To compare the effects of rehabilitation on the flexural behaviour of RCC beams, twelve beam specimens were cast and subjected to four point bending, before and after strengthening with equivalent laminates of CFRP, GFRP

*Corresponding author, Former Professor and Head
E-mail: ganesan@nitc.ac.in
[a]Ph.D. Student
E-mail: binduranip@gmail.com
[b]Professor and Head
E-mail: indira@nitc.ac.in

http://www.techno-press.org/?journal=acc&subpage=7 ISSN: 2287-5301 (Print), 2287-531X (Online)

and ferrocement. The beams were subjected to different levels of pre-distress (the term pre-distress in this study emphasises the distress induced deliberately to the specimens prior to rehabilitation), and the failure modes, the crack width patterns, load-deflection behavior and moment-curvature relationships were studied.

2. Experimental programme

The experimental programme was conducted in two phases. The first phase comprised of finding the equivalent laminates of ferrocement and FRPs, which were used for strengthening the RCC beam specimens. The flexural strength of any composite depends on the tensile strength of the same. Since failure occurs in the composite as and when the tensile stress exceeds the modulus of rupture of this material. Hence the laminates were equated in terms of its tensile strength since this mechanical property is mainly contributing to the flexural strengthening of beams. For this purpose unidirectional tensile tests were conducted on similar coupons of FRPs and ferrocement with varying number of layers in order to find the coupons with equivalent tensile strengths. The second phase consisted of casting of twelve RCC beam specimens and testing before and after rehabilitation using the equivalent laminates. The beam specimens were sorted into three groups with four beams in each group. The beams in each group were induced with different levels of distress before the strengthening process. The beams were subjected to four point bending in order to induce the pre-distress. The parameters considered in this study were the levels of pre-distress and the composites for rehabilitation.

2.1 Phase 1: Material tensile tests

2.1.1 Materials used and test coupons

The CFRP composite selected in this study consists of unidirectional carbon fibre woven mat (CERA CFR MEMBRANE 230 2017; see Fig. 1(a)) of weight 230g/sqm impregnated in epoxy resin. Similarly, GFRP consists of bi-directionally woven glass fibre mat (EW200 (200±20gsm) n.d.; see Fig. 1(b)) of weight 220g/sqm impregnated in the same resin material. The epoxy resin used for making both kinds of FRP was a two-part system (CERA PRIMER EP S 2013) of base and hardener which was combined in a mix proportion of 5:3 by weight. For preparing the FRP composites, the fibre and the resin were taken in a ratio of 1:1 by weight.

The ferrocement was made of Portland pozzolana cement (PPC, 53 grade), manufactured sand (*M* sand) which passes through 2.36 mm IS sieve, potable water and wire mesh. The 28th day compressive strength of 1:2 cement-sand mortar with water/cement ratio 0.5 by weight was 53.19 MPa. The wire mesh used in this study was a locally available galvanized iron (GI) square woven mesh of gauge 12/29, having a mesh size of 2.12 mm with 0.35 mm diameter wires (see Fig. 1(c)). As the cement mortar is weak in tension, the tensile strength of ferrocement is contributed mostly by the wire mesh alone. Hence, for making the ferrocement tensile test coupons for the phase 1 experimental study, the wire mesh alone was used as mentioned in ACI 549.1R-93 (1999). The technical properties of the selected materials are consolidated in Table 1.

The tensile tests were conducted as per ASTM D3039/D3039M (2000). Test coupons of width 25 mm and length 280 mm were fabricated by following the wet lay-up procedure given in ASTM D7565/D7565M (2017) for the FRP materials. 300 mm×300 mm laminate sheets were prepared as per the given procedure, cured at ambient temperature for a few days and then cut the required sized coupons. By following the recommendations given in ASTM D3039 (2000), two flat rectangular aluminium tabs of thickness 1.5 mm, width 30 mm and length 80 mm were glued on the opposite faces of the test coupons at each end to prevent the gripping damage, as well as to ensure that the failure occurs within the fibre direction while testing.

For ferrocement tension specimens, coupons of wire mesh having layers of wire mesh strips with a width 25 mm and length 280 mm were prepared by cutting the wire mesh sheet. The width and the length were so selected to match with those of FRP coupons. Similar aluminium tabs were used for ferrocement coupons also to avoid failure within the grips.

A total of fifty-five tension specimens were prepared from the three different materials, out of which ten from CFRP, twenty-five from GFRP and twenty from wire mesh; with a different number of layers, and were sorted into groups. CFRP was tested in two groups with one and two layers, GFRP was tested in five groups with the number of layers varies from two to six, and the wire mesh coupons were tested in four groups having three to six layers. In each group, five sample specimens were made and tested as per ASTM D3039 (2000), which recommends testing of at least five samples per test condition to get a reliable result. Typical test coupons from the three different materials are shown in Fig. 2.

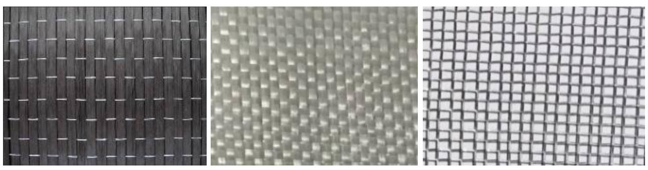

(a) Woven carbon fibre mat (b) Woven glass fibre mat (c) Woven GI wire mesh

Fig. 1 Materials selected for rehabilitation

Table 1 Technical properties of the materials

Properties	Carbon fibre mat	Glass fibre mat	GI Wiremesh of ferrocement
Width (mm)	500	900	1000
Dry fabric thickness (mm)	0.21	0.18	0.54
Tensile Modulus (GPa)	230	160	90
Tensile Strength (MPa)	3900	3500	425
Total weight of sheet (g/m^2)	230	220	590
Density (g/cm^3)	1.8	1.7	7.85

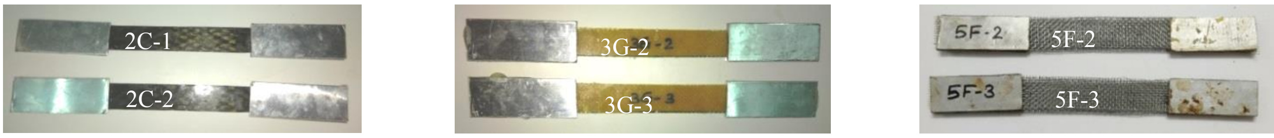

(a) CFRP (b) GFRP (c) Wire mesh of ferrocement

Fig. 2 Typical tension test coupons

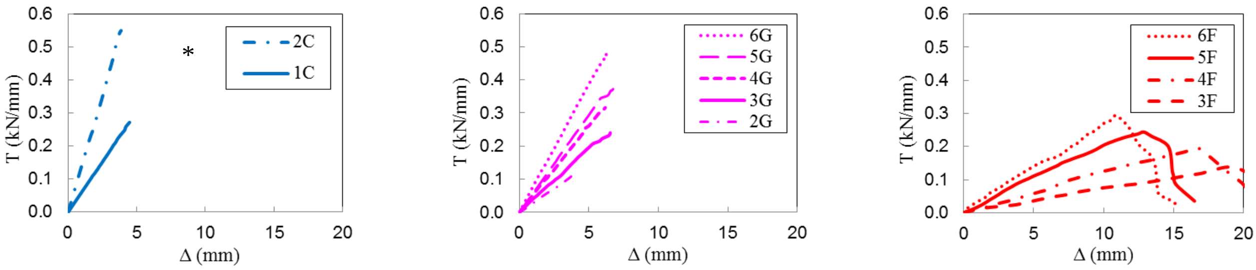

(a) CFRP (b) GFRP (c) Wire mesh of ferrocement

* 1C:1 layer of CFRP; 2G: 2 layers of GFRP; 3F: 3 layers of wire mesh of ferrocement

Fig. 3 Tensile force/unit width versus elongation of tension coupons with various numbers of layers

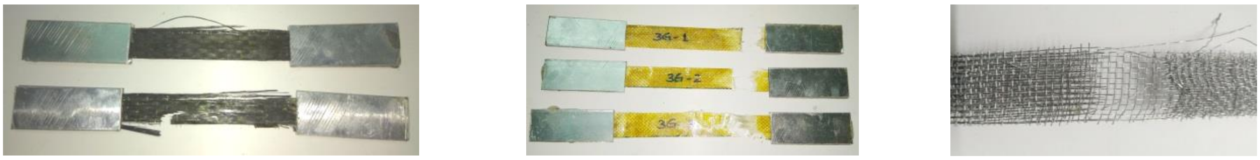

(a) CFRP (b) GFRP (c) Wire mesh of ferrocement

Fig. 4 Failure modes in test coupons

The coupons were named such that the names include the number of layers used, material representation (namely C: CFRP, G: GFRP, F: ferrocement) and the sample number. For example, 3G-2 represents the second specimen in the group of glass laminate with 3 layers.

2.1.2 Results of tensile tests

The tension tests were conducted in a universal testing machine (model UTM-2011N), having a capacity of 200 kN. The specimen was kept between the fixed and movable serrated jaws of the machine such that the longitudinal axis of the gripped specimen aligned with the test direction. Also, it was placed such that the grip jaws extended approximately 15 mm past the inner ends of tabs, to prevent failure at the tab ends due to excessive inter-laminar stresses.

The load was applied to the specimen at a constant rate with a standard head displacement rate of 2 mm/min, such that the failure occurs within 1 to 10 minutes as specified in ASTM D3039 (2000). Loads and the corresponding elongations were noted from the machine at intervals of 0.2kN, and depicted in a graphical form in Figs. 3(a)-(c), with elongation (Δ) in the X axis and tensile force/unit width (T) in the Y axis. The load at failure of each specimen was recorded. Failure modes were noted and it was seen that almost all the failures happened in the gauge region, which is the recommended type as per ASTM D3039 (2000). For CFRP specimens, long splitting and edge delamination in the middle gauge zone were the predominant modes of failure, while in GFRP, lateral or angled breaking failures were predominant. For wire mesh specimens, the failure modes in all specimens were yielding and breaking of one or more layers within the gauge region. Some of the failed specimens are shown in Figs. 4(a)-(c).

Table 2 Tensile strength (N/mm) of test coupons with various numbers of layers

Number of layers	CFRP	GFRP	Wiremesh of Ferrocement
1	**246.71**	-	-
2	541.24	118.43	-
3	-	**242.10**	136.43
4	-	312.46	194.01
5	-	389.96	**243.90**
6	-	487.65	292.06

The maximum tensile force per unit width for the specimens in each group was calculated by following the recommendations in ASTM D7565 (2017). The average tensile force per unit width for each group of plies was calculated and represented in Table 2. From the experimental results, the average tensile force per unit width for 1 layer CFRP, 3 layer GFRP and 5 layer wire mesh coupons were 246.71 N/mm, 242.1 N/mm and 243.9 N/mm, which were comparatively equal.

From the phase 1 study it was found that, for the selected constituents of FRP and ferrocement composites, CFRP with 1 layer is equivalent to (i) GFRP with 3 layers and (ii) ferrocement with 5 layers of wire mesh reinforcement, in terms of tensile strength. Hence these equivalent laminates were used in the phase 2 study.

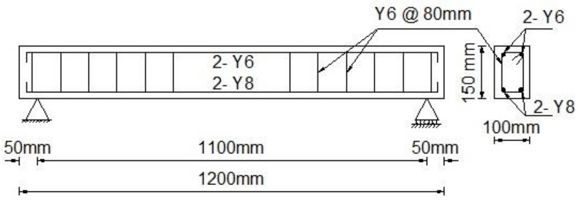

Fig. 5 Details of beam specimen

2.2 Phase 2: Flexural tests of RCC beams rehabilitated with equivalent composites

2.2.1 Details of beam specimens

A total of twelve RCC beams, having a size of 100 mm in width, 150 mm in depth and an overall length of 1200 mm were cast using PPC, M sand as fine aggregate, 12 mm crushed stone as coarse aggregate, water, and high yield strength deformed (HYSD) bars with diameters 8 mm and 6 mm as reinforcement. The PPC used was of grade 53 and having a specific gravity 3.05. M-sand, passed through 4.75 mm IS sieve and conforming to grading zone II as per IS 383 (2016), had a specific gravity 2.53 and fineness modulus 2.81. The coarse aggregate had a specific gravity of 2.7 and fineness modulus of 7.05. The concrete used for casting the RCC specimens was of M35 grade and designed as per IS 456 (2000) and IS 10262 (2009). The 28th-day compressive strength obtained by a mix proportion of 1:1.55:2.78 with water/cement ratio 0.5 by weight was 35.6MPa. The slump obtained for this mix was 65mm.

The beam specimen was designed as under reinforced with longitudinal reinforcement of two 8mm diameter HYSD bars (designated with "*Y*") at the bottom as tension reinforcement and two 6mm diameter bars at the top as stirrup holders. Two-legged stirrups of 6mm diameter bars @ 80 mm *c/c* were provided at the shear span region with a clear cover of 20 mm. The shear reinforcement was designed to ensure the flexural failure of the beams. The yield strength of HYSD bars used were 571 MPa and 499 MPa for 8 mm and 6mm diameter bars respectively. The same reinforcement details were followed for all the beam specimens. Fig. 5 depicts the details of the specimen.

2.2.2 Test set-up

After casting, the specimens were water cured for 28 days. Then these twelve specimens were sorted into three groups of four beams each. From each group, one beam was tested up to failure to find the ultimate load and that was kept as a control beam (CB). Other beams were preloaded to 70%, 80% and 90% of the ultimate load and the cracking behaviour in all these beams was observed. The first group of beams was then rehabilitated with 1 layer of CFRP laminate. Similarly, the other two groups of beams were induced to have distress as explained earlier. The preloaded Group-2 beams were rehabilitated with 3 layers of GFRP, and Group-3 beams with 5 layers of ferrocement. The 100% preloaded control beams in each group were also rehabilitated with the corresponding composites to understand the extent of rehabilitation potentials of the selected composites.

Four point bending scheme was selected for testing

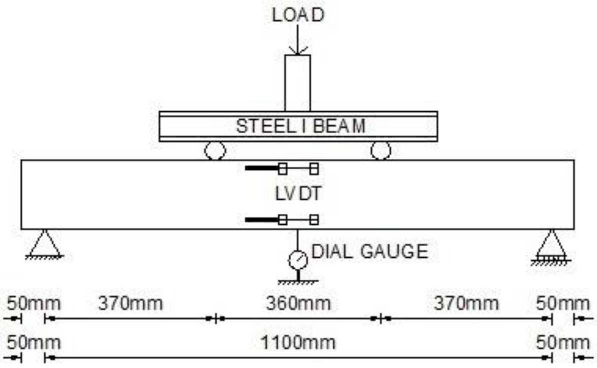

(a) Schematic diagram

(b) Actual set-up showing LVDT and load indicator

Fig. 6 Test set-up

since it results a constant maximum moment and zero shear at the middle portion of the beams between the loading points which indicates a pure bending condition. The beams were preloaded in a universal testing machine (UTM) of 3000 kN capacity. The span was kept as 1100 mm between the supports. A dial gauge was placed to touch the soffit of the beam at the centre of the span to measure the mid-span deflection. Two linear variable differential transformers (LVDT) were placed at the top and bottom of the mid-span of the beam to measure the deformations at the compression and tension zones respectively with a gauge length of 100mm. Both the deflection and strain measurements were noted at a load interval of 1 kN. The load was applied monotonically at a rate of 3 kN/min for all the specimens. Figs. 6 (a)-(b) show the schematic and the actual test set up. The same test set up was followed for testing the beams prior to and after rehabilitation.

2.2.3 Pre-loading of specimens prior to rehabilitation

The twelve beam specimens were sorted into three groups of four beams each, viz. Group-1 to Group-3 which meant for rehabilitation using CFRP, GFRP, and ferrocement respectively. In each group, one beam was tested to failure (100%) to find the ultimate load. Since the testing was done in a load controlled UTM, it was difficult to monitor the deflection after reaching the peak load. So the control beam in each of the three groups was unloaded at 85% of the peak load in the post-peak load-deflection curve. The distress at this level was defined as the 100% distress level and the corresponding load was defined as the

(a) Control beam (100% distress)

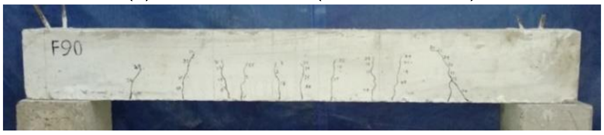

(b) 90% distressed beam

(c) 80% distressed beam

(d) 70% distressed beam

Fig. 7 Typical distressed beams prior to rehabilitation

failure load (i.e., 85% of the peak load) in this study. The rest of the specimens in each group were preloaded up to 70%, 80% and 90% of the ultimate load and was referred as beams at respective distress level. Fig. 7 shows some typical pre-loaded beams before being rehabilitated from all the groups. The pre-loading levels were adopted to simulate the loading conditions above the service load condition. The first cracking load and crack patterns were noted during pre-loading (i.e., prior to rehabilitation). It was noticed that all the beams showed the standard flexural cracks in the middle portion of the beam. The first cracking load was either 4 kN or 5 kN for all the beams, which shows that all the beams were of almost the same strength.

2.2.4 Rehabilitation of distressed specimens using equivalent composites

The distressed specimens were rehabilitated using equivalent composites of CFRP, GFRP, and ferrocement. For flexural strengthening, one of the options is to provide the laminates at the soffit of the beam (Patel *et al*. 2015). Here, the FRP laminates were attached to the soffit of the Group-1 and Group-2 distressed beams by wet lay-up procedure and ferrocement laminates to Group-3 beams by in-situ application. Fig. 8 shows the schematic representation of the position of the laminate on the distressed beams. The size of the laminates was selected to fit between the supports. The laminates act as additional tension reinforcement to the beams.

Before the application of these strengthening composites, the soffits of the distressed beams were prepared for having sufficient bond between the composites and the substrate surface. For FRP rehabilitation, profiling of concrete surface is very important as bonding is greatly influenced by surface preparation (ACI 546R 2014). Since the width of the cracks observed was less than 0.35 mm, loose concrete was not encountered. The concrete was

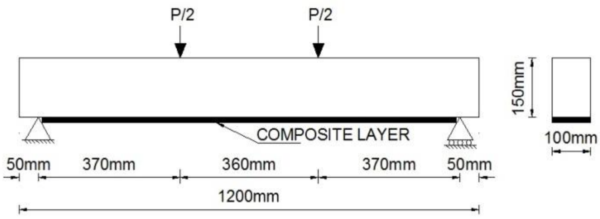

Fig. 8 Beam with composite laminate at soffit for strengthening

(a) Prepared beam soffit for FRP application (upside-down view)

(b) Primed beam soffit

(c) Cut strips of glass fibre mat

(d) Impregnating FRP strips in epoxy resin

Fig. 9 Pictures of FRP rehabilitation process

sound between the cracks as the specimens were freshly prepared. A concrete surface profile similar to CSP 3 as per ICRI 310.2R (2013) was achieved (see Fig. 9(a)) by thoroughly cleaning the beam soffits by brushing and water jetting. Epoxy primer (CERA PRIMER EP 18 2013) was then applied over this prepared beam soffits and the cracks were filled using the same primer which resulted in a smooth surface after curing (see Fig. 9(b)). The primed specimens were cured for a day at room temperature (i.e., 28°C average) before the application of FRP laminates. The

(a) Chiseled beam soffit (upside-down view)

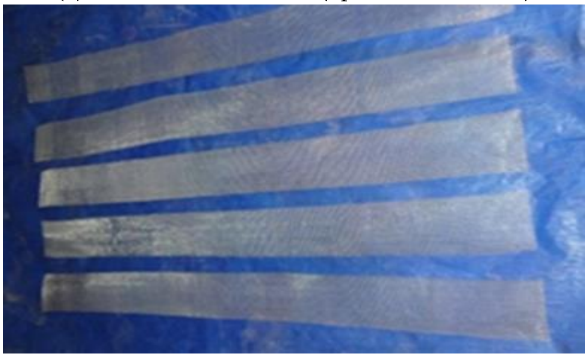

(b) Cut strips of wire meshes

(c) Wire mesh tied over the grouted specimen (upside-down view)

Fig. 10 Pictures of ferrocement rehabilitation process

primer selected was a two-part system of base and hardener which was mixed in a proportion of 2:1 by weight. For ferrocement rehabilitation, the soffits of Group-3 beams were roughened by chiseling to have a proper bond with ferrocement laminate (see Fig. 10(a)).

The CFRP and GFRP sheets were cut to the required size (see Fig. 9(c)) and were impregnated in the prepared epoxy resin (see Fig. 9(d)) to get the laminates for Group-1 and Group-2 respectively. These impregnated laminates were applied immediately over the primed and cured surfaces of the specimens and pressed with a paint roller to bond it firmly to the surface. Required number of resin-saturated FRP strips were placed successively over the previous layer and pressed with the roller. The excess matrix and entrapped air were removed with a flat scraping blade.

For ferrocement rehabilitation, 5 layers of wire meshes were cut with the required size (see Fig. 10(b)) and tied to the soffit of the beam after applying a rich cement paste at the soffit (see Fig. 10(c)). The wire mesh strips were tied one after the other using the same type of GI wire running around the specimen at an approximate spacing of 200 mm. Cement sand mortar of 1:2 ratio by weight with water-cement ratio 0.5 was prepared and applied over the wire mesh. A thin layer of mortar was applied between each layer of wire mesh to ensure bonding and finished the entire laminate to an approximate uniform thickness of 15 mm.

(a) Distressed beam rehabilitated with 1 layer CFRP

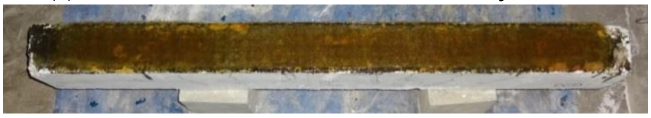

(b) Distressed beam rehabilitated with 3 layer GFRP

(c) Distressed beam rehabilitated with ferrocement having 5 layers of wire mesh reinforcement

Fig. 11 Distressed beams with composite laminate at soffit to attain flexural strength (upside-down views)

Figs. 11(a)-(c) show the specimens rehabilitated with 1 layer of CFRP, 3 layers of GFRP and ferrocement having 5 layers of wire mesh reinforcement respectively.

All the strengthened specimens were cured for two weeks so that they were completely hardened before testing. FRP strengthened specimens were cured at ambient temperature (i.e., room temperature that varied between 30±2°C and 23±2°C) and the ferrocement strengthened specimens were water cured by covering with wet jute sacks. The cured specimens were tested in the UTM under four-point bending with the test set-up explained in Section 2.2.2. All the rehabilitated specimens were tested up to the failure to find the ultimate load carrying capacity. Before testing, the specimens were whitewashed at the sides to view the new crack development. The mid-span deflections corresponding to a load interval of 1 kN were noted till failure. LVDTs, having a least count of 0.01 mm, were used to take the axial displacements at the tension and compression zones of the beams at the mid-span region. The rate of loading was kept the same as 3 kN/min.

The specimens were named appropriately and their designation contains (i) the material code (viz. *C*, *G*, and *F* respectively for CFRP, GFRP, and ferrocement), (ii) amount of pre-distress (viz. 100, 90, 80 and 70 respectively for corresponding percentage of distress) and (iii) the status of rehabilitation (viz. PR for prior to rehabilitation and *R* for after rehabilitation). For example, C70_R represents the beam specimen pre-distressed up to 70% of the ultimate load, rehabilitated with CFRP laminate.

3. Test results and discussions

3.1 Cracking behaviour and ultimate loads

All the three groups of rehabilitated beams showed a similar, flexural cracking behaviour with the development of flexural cracks in the middle span region which propagated up the beam. As the load increased, the spacing of the cracks decreased and some cracks joined together and

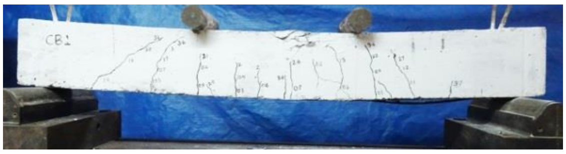

(a) Beam rehabilitated at 100% distress (C100_R)

(b) Beam rehabilitated at 90% distress (C90_R)

(c) Beam rehabilitated at 80% distress (C80_R)

(d) Beam rehabilitated at 70% distress (C70_R)

Fig. 12 Crack patterns in the rehabilitated beams strengthened with 1 layer CFRP laminate (Group-1)

(a) Beam rehabilitated at 100% distress (G100_R)

(b) Beam rehabilitated at 90% distress (G90_R)

(c) Beam rehabilitated at 80% distress (G80_R)

(d) Beam rehabilitated at 70% distress (G70_R)

Fig. 13 Crack patterns in the rehabilitated beams strengthened with 3 layer GFRP laminate (Group-2)

yielding of steel reinforcement within the beam transferred a portion of the tensile load to the reinforcing laminate. Ultimately the beam failed due to rupture of the laminate near the crack, or due to debonding initiated by flexural

(a) Beam rehabilitated at 100% distress (F100_R)

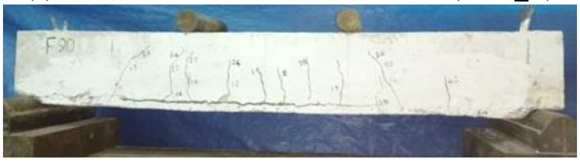

(b) Beam rehabilitated at 90% distress (F90_R)

(c) Beam rehabilitated at 80% distress (F80_R)

(d) Beam rehabilitated at 70% distress (F70_R)

Fig. 14 Crack patterns in the rehabilitated beams strengthened with 5 layer ferrocement laminate (Group-3)

cracks. The failure patterns of the rehabilitated beams in Groups 1-3 are shown in Figs. 12-14 respectively. Table 3 shows the values of cracking loads, ultimate loads and corresponding deflections along with the failure modes. It also lists the maximum applied load and corresponding deflection at each distress level of the beams before being rehabilitated.

Three types of failure patterns were observed in FRP strengthened beams, viz. debonding, delamination and rupture of laminates. The debonding initiated at the midspan near cracks and extended towards the end of the beam, which leads to the total debonding of the laminate (see Fig. 12(d)). Also a peeling type of failure of the cover concrete at the level of steel reinforcement occurred, and the cover concrete got detached along with the laminates (see Fig. 12(b)). One specimen showed a cover delamination failure at the curtailment of bonded FRP laminate which initiated by a flexure-shear crack (see Fig. 12(c)). Rupture and long splitting of CFRP laminate were also observed in this specimen. All the GFRP strengthened specimens experienced more deformations at the ultimate load than the CFRP strengthened specimens and failed due to rupture of the GFRP laminate (see Fig. 13). GFRP's high deformability (low material stiffness) allowed it to reach the rupture strain at failure. Most of the observed failure modes were similar to those observed in the tensile coupon tests for obtaining the equivalent strength laminates (see Section 2.1.2). These were long splitting or edge delamination type of failure for CFRP and breaking failure for GFRP laminates.

Ferrocement rehabilitated specimens (see Fig. 14), also failed in flexure. As the load increased, the flexure cracks at

Table 3 Test results prior to and after rehabilitation

Specimen group no.	Beam designation	% Distress level	First crack load (kN)		Ultimate load/ Maximum applied load (kN)		Deflection corresponding to ultimate load (mm)		Failure Mode (R)
			PR*	R	PR	R	PR	R	
1 (CFRP rehabilitated)	C100	100	4	4	39	44	8.70	9.68	Debonding initiated by flexure cracks
	C90	90	4	5	36	56	6.18	10.65	
	C80	80	4	5	32	61	4.96	10.93	
	C70	70	4	6	28	67	4.02	12.08	
2 (GFRP rehabilitated)	G100	100	5	4	40	45	9.80	12.25	Rupture of GFRP laminate
	G90	90	4	4	36	52	6.25	12.84	
	G80	80	4	4	32	58	4.95	12.40	
	G70	70	5	6	28	62	4.14	12.85	
3 (Ferrocement rehabilitated)	F100	100	5	6	40	54	9.50	10.90	Debonding initiated by flexure cracks
	F90	90	4	6	36	55	5.29	12.00	
	F80	80	4	4	32	60	4.55	11.41	
	F70	70	4	6	28	66	3.93	12.95	

*PR: Prior to Rehabilitation; R: after Rehabilitation

the midspan region gradually increased in size and numbers, through the laminate and extended towards the top of the original beam. After attaining the ultimate load, a bonding failure was observed in these beams and the specimens finally failed due to the delamination of the laminate.

In the case of rehabilitated specimens, the first cracking occurred at the same or slightly higher load when compared to control specimens. For all the strengthened specimens, the ultimate load was found to be higher than the control specimens.

3.2 Load-deflection behaviour

Load-deflection (F-δ) behaviour was plotted for the beams rehabilitated with the same material at different levels of pre-distress and are shown in Figs. 15(a)-(c). All the graphs include the corresponding control beam for having a reference.

It may be observed from the figures that the load carrying capacity of all the specimens were improved due to rehabilitation, irrespective of the pre-distress level, and the percentage increase was more with lower levels of pre-distress. All three control beams performed in a similar manner with less than 10% variation in the test data. The control beam F100_CB, which performed in an average manner among the three, was selected as the reference control beam. This was used for the comparison of different rehabilitation schemes at the same level of pre-distress, except at 100% level (where the data was available for the same beam before and after rehabilitation). The percentage increase in the load carrying capacity of the strengthened specimens from the control specimens is depicted in Fig. 16. The CFRP rehabilitated specimens showed an increase in load carrying capacity from 12.8% to 67.5% as the distress level lowers from 100% to 70%. For GFRP rehabilitated specimens, a similar increase was 12.5% to 55% and for ferrocement rehabilitated beams, it was 35% to 65%. When the ferrocement rehabilitation scheme was compared with FRP schemes, it was seen that ferrocement

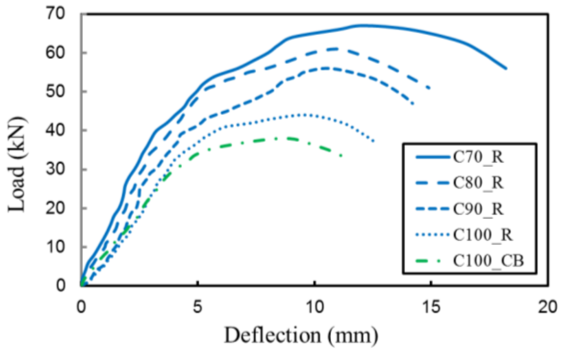

(a) CFRP rehabilitated beams versus control beam

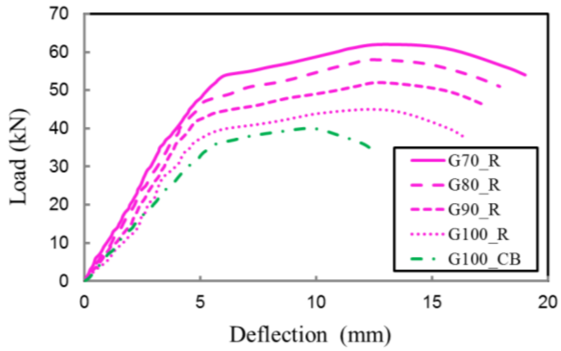

(b) GFRP rehabilitated beams versus control beam

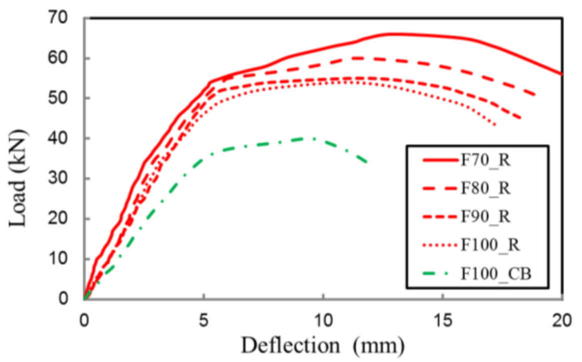

(c) Ferrocement rehabilitated beams versus control beam

Fig. 15 Load-deflection behavior of beams rehabilitated with the selected material

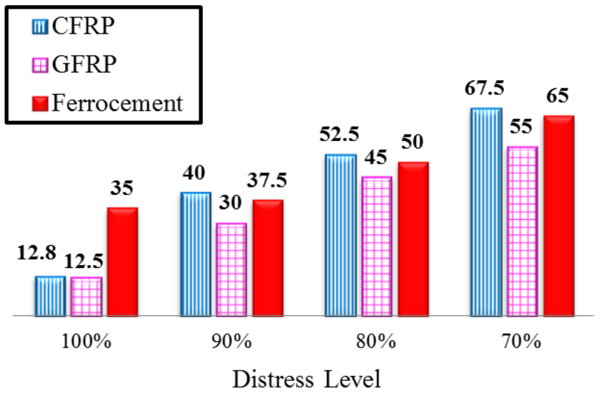

Fig. 16 Percentage increase of load carrying capacity compared to control specimen

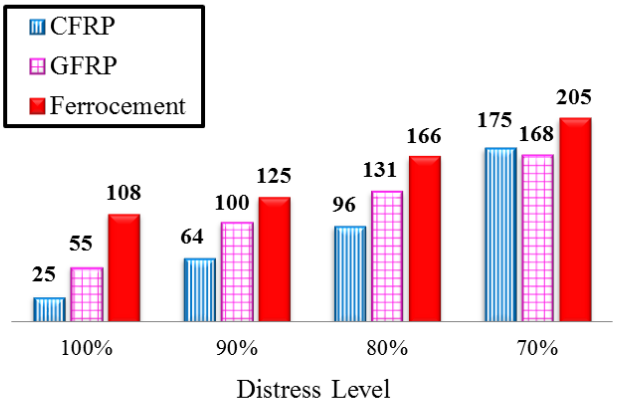

Fig. 17 Percentage increase of energy absorption capacity compared to control specimen

closely followed CFRP at all the pre-distress levels except at 100% (where it showed a better performance), and it outperformed GFRP at all the levels of pre-distress. This dependency of the ultimate load capacity on the pre-loading levels was also observed by Ebead (2015).

Energy absorption capacity explains the performance of the specimens in a better way, and it can be determined by calculating the area under the load-deflection curves. Due to the limitations of the test set-up, the load-deflections curves could be plotted up to the failure load (i.e. 85% of peak load) in the post-peak region. The energy absorption capacities and the displacement ductility indices of the rehabilitated specimens were calculated and are shown in Table 4. Fig. 17 shows the percentage increase in the energy absorption capacity of the rehabilitated beams with respect to the control beams. The percentage increase in the energy absorption capacity of a strengthened beam varies inversely to the amount of pre-distress irrespective of the selected material used for strengthening. Out of the three selected composites, ferrocement exhibits a better percentage increase in the energy absorption capacity above the control specimen (108% to 205%) than CFRP (25% to 195%) and GFRP (55% to 157%), for a pre-distress level variation from 100% to 70%.

For calculating the displacement ductility index and the flexural stiffness, the yield load was determined by drawing trilinear fitted lines on the corresponding load-deflection

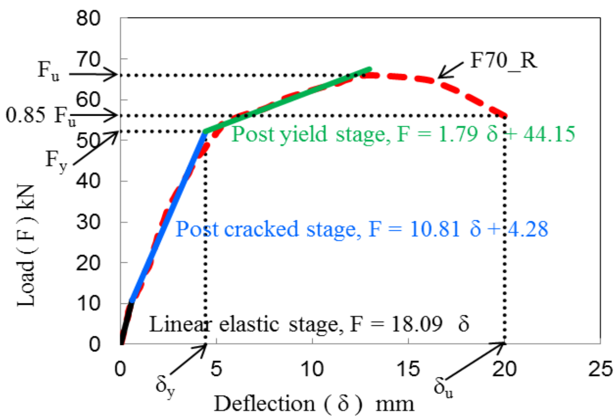

Fig. 18 Typical trilinear plot defining yield point in the load-deflection curve of F70_R

curves. Fig. 18 depicts a typical trilinear fitted line plot corresponding to the experimental curve, which was used to define the yield point. The flexural stiffness at various loading stages was obtained from these plots. The linear elastic stage in the curves was very small since the beams were pre-distressed. The slope of the trilinear plot at its second and third lines gave the flexural stiffness at the pre-yield and post-yield stages respectively. Table 5 shows the flexural stiffness values and its percentage increase from the typical control beam (F100_CB). It is seen that as the pre-distress levels increases (70% to 100%) the percentage increase in attainment of pre-yield stiffness decreases rapidly for CFRP (49% to 14%), but the ferrocement rehabilitated specimens maintained an almost same flexural stiffness irrespective of the pre-distress levels (56% to 50%). GFRP possessed a lower stiffness than the other two schemes at almost all pre-distress levels. Even though the ultimate load achieved was more for CFRP strengthened specimens for most pre-distress levels, the performance of ferrocement rehabilitation appeared to be more consistent in the pre-yield stage when compared to FRPs. The load-deflections curves for ferrocement and GFRP appeared smoother than CFRP; the difference in the behavior of CFRP strengthening might be due to the “intermediate crack induced debonding” type of failure mentioned by Teng *et al*. (2003), Tahsiri *et al*. (2015).

The displacement ductility factor (ψ; see Table 4) was calculated using Eq. (1) in which δ_y was the deflection corresponding to the yield load (F_u), and δ_u was that corresponding to failure load ($0.85F_u$ at the post-peak curve).

$$\psi = \frac{\delta_u}{\delta_y} \tag{1}$$

The relative displacement ductility of ferrocement is higher than that of GFRP and CFRP at each level of pre-distress (see Table 4), which is quite evident due to the brittle nature of FRP. Between the two FRP systems, GFRP exhibits a better ductility than CFRP at higher pre-distress levels. For CFRP strengthening, the ductility drastically decreased (1.53 to 0.96) as the levels of pre-distress increased.

Table 4 Energy absorption capacity and displacement ductility

Specimen group no.	Beam designation	% Distress level	Energy absorption capacity (kN-m)	Deflection (mm)		Displacement ductility factor $\psi=\delta_u/\delta_y$	
				δ_y	δ_u	Absolute	Relative
1 (CFRP rehabilitated)	C100_CB*	100	0.328	4.29	11.50	2.68	1.00
	C100_R	100	0.409	4.90	12.60	2.57	0.96
	C90_R	90	0.576	5.27	14.20	2.69	1.01
	C80_R	80	0.689	4.94	14.90	3.02	1.13
	C70_R	70	0.967	4.43	18.20	4.11	1.53
2 (GFRP rehabilitated)	G100_CB	100	0.367	5.07	12.40	2.45	1.00
	G100_R	100	0.568	5.14	16.30	3.17	1.30
	G90_R	90	0.703	5.12	17.30	3.38	1.38
	G80_R	80	0.814	5.17	17.90	3.46	1.42
	G70_R	70	0.942	5.23	19.00	3.63	1.49
3 (Ferrocement rehabilitated)	F100_CB	100	0.352	4.57	11.85	2.59	1.00
	F100_R	100	0.733	4.51	16.80	3.73	1.44
	F90_R	90	0.793	4.66	17.60	3.78	1.46
	F80_R	80	0.938	4.76	19.20	4.03	1.56
	F70_R	70	1.075	4.42	20.00	4.53	1.75

*CB: Control Beam; R: beam after Rehabilitation

3.3 Moment-curvature relationship

The distribution of moments and strains in the beam section is represented by the moment-curvature relationships of the specimens. The curvature was calculated from the strains on the concrete surface at the compression and tension faces at the midspan location. The strain values were obtained from the linear deformations measured using LVDTs, those placed at a gauge length (GL) of 100 mm. The compressive strain (ε_c) and the tensile strain (ε_s) were calculated as follows.

$$\varepsilon_c = \frac{\Delta_c}{GL} \tag{2}$$

$$\varepsilon_s = \frac{\Delta_s}{GL} \tag{3}$$

where Δ_c and Δ_s were the LVDT readings at compression and tension zones. The curvature (ϕ) was obtained from the following relation, in which d was the effective depth of the beam.

$$\Phi = \frac{\varepsilon_c + \varepsilon_s}{d} \tag{4}$$

The corresponding moment (M) was calculated from the applied loads (F) using the relation Eq. (5) which is relevant to the loading configuration shown in Fig. 6(a).

$$M = 0.185F \tag{5}$$

The moment-curvature relationships of the beams rehabilitated with the selected equivalent composites at the same level of pre-distress are shown in Figs. 19(a)-(d). The curvatures and the curvature ductility indices were calculated from the moment-curvature curves and are represented in Table 6. To avoid congestion in these plots, only a typical control beam (F100_CB) was shown as reference for comparison. It is clear from the curves that the curvatures were less at the same moments for the strengthened beams than the typical control beam if the amount of pre-distress is lower than 80%.

Table 5 Flexural stiffness

Specimen group no.	Beam designation	% Distress level	Flexural stiffness			
			Pre-yield stage		Post-yield stage	
			(kN/mm)	% increase	(kN/mm)	% increase
1 (CFRP rehabilitated)	C100_CB	100	7.55	-	0.98	-
	C100_R	100	8.57	14	1.13	15
	C90_R	90	9.88	33	2.74	204
	C80_R	80	10.49	41	1.92	113
	C70_R	70	11.08	49	2.01	123
2 (GFRP rehabilitated)	G100_CB	100	6.72	-	0.96	-
	G100_R	100	8.30	24	0.98	2
	G90_R	90	9.52	28	1.20	33
	G80_R	80	9.83	32	1.49	66
	G70_R	70	10.01	34	1.59	77
3 (Ferrocement rehabilitated)	F100_CB	100	7.45	-	0.90	-
	F100_R	100	11.14	50	0.91	1
	F90_R	90	11.22	51	0.85	-6
	F80_R	80	11.49	54	0.93	3
	F70_R	70	11.61	56	1.79	99

The yield point in the plots was defined in the same manner as shown in Fig. 18 by drawing trilinear fitted lines for the moment-curvature plots. Eq. (6) was used to calculate the ductility index (μ), where ϕ_y was the curvature corresponding to the yield point and ϕ_u was that corresponding to 85% of the peak moment in the post-peak moment-curvature curve.

$$\mu = \frac{\Phi_u}{\Phi_y} \tag{6}$$

Both the ferrocement and GFRP rehabilitated beams exhibit higher curvature ductility (more than 2) at lower

Table 6 Curvature ductility

Specimen group no.	Beam Designation	% Distress level	Curvature ($\times 10^{-3}$ rad/m)		Curvature ductility index, $\mu = \phi_u/\phi_y$	
			ϕ_u	ϕ_y	Absolute	Relative
1 (CFRP rehabilitated)	C100_CB	100	0.087	0.051	1.71	1.00
	C100_R	100	0.167	0.075	2.23	1.30
	C90_R	90	0.195	0.080	2.44	1.43
	C80_R	80	0.194	0.083	2.34	1.37
	C70_R	70	0.210	0.096	2.19	1.28
2 (GFRP rehabilitated)	G100_CB	100	0.088	0.047	1.87	1.00
	G100_R	100	0.210	0.089	2.36	1.26
	G90_R	90	0.221	0.091	2.43	1.30
	G80_R	80	0.232	0.062	3.74	2.00
	G70_R	70	0.224	0.053	4.23	2.26
3 (Ferrocement rehabilitated)	F100_CB	100	0.094	0.050	1.88	1.00
	F100_R	100	0.215	0.100	2.15	1.14
	F90_R	90	0.230	0.068	3.38	1.80
	F80_R	80	0.245	0.061	4.02	2.14
	F70_R	70	0.248	0.060	4.13	2.20

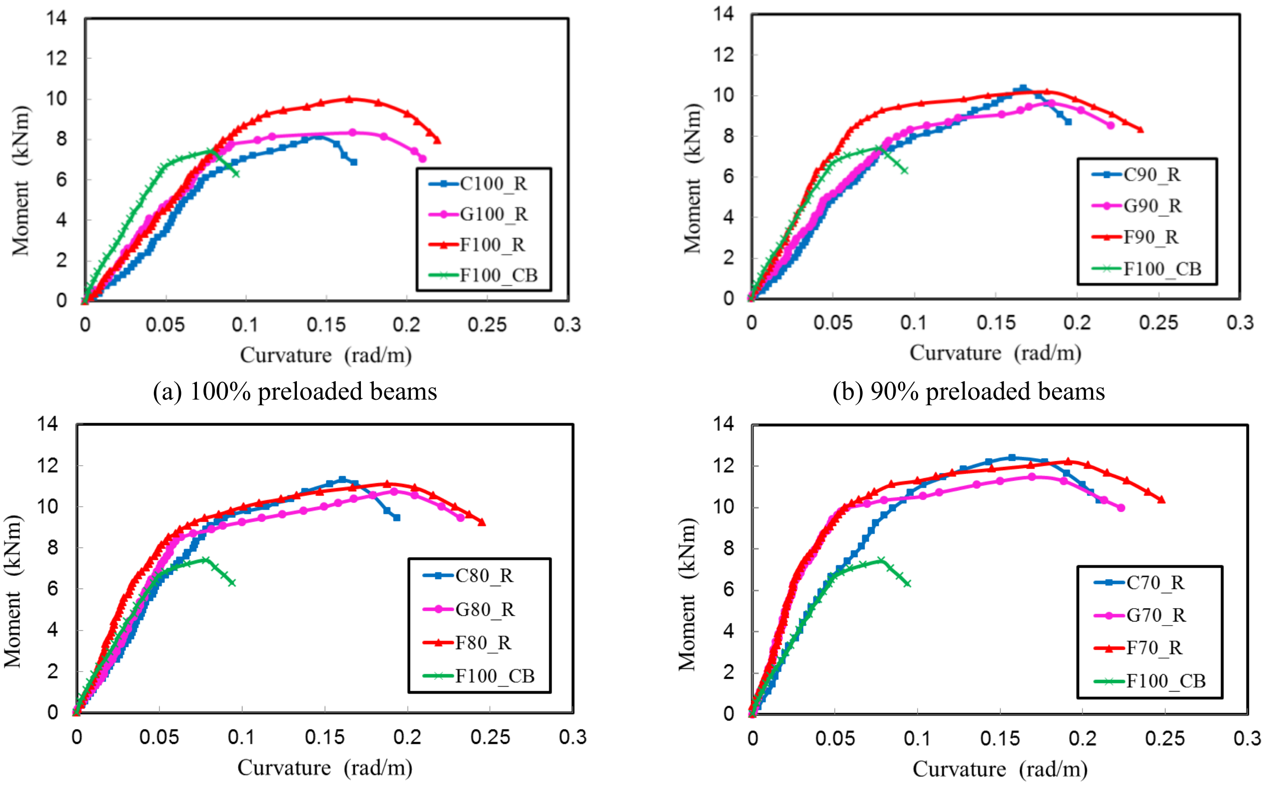

(a) 100% preloaded beams (b) 90% preloaded beams

(c) 80% preloaded beams (d) 70% preloaded beams

Fig. 19 Moment-curvature behavior of rehabilitated beams compared at different distress levels

levels of pre-distress (i.e., less than 80%), which represents the ability of these specimens to undergo higher inelastic deformations without much reduction in strength. The curvatures at the ultimate load for ferrocement rehabilitation showed the higher values which closely followed by GFRP rehabilitation and CFRP showed the least values. Hence, between the FRPs, CFRP appeared to be more brittle than equivalent GFRP. Also, the CFRP rehabilitated specimens showed a more or less same ductility at all levels of pre-distress (i.e., between 1.28 and 1.43). But for GFRP and ferrocement, the curvature ductility increased with reduction in the pre-distress levels (1.26 to 2.26 for GFRP and 1.14 to 2.2 for ferrocement).

3.4 Crack width analysis

During loading, for the rehabilitated beams, the widths of all the new cracks were measured at intervals and were plotted against the load as shown in Figs. 20(a)-(d). A large number of new cracks formed after rehabilitation. The crack widths were also measured for all the control beams tested prior to rehabilitation and all of them appeared to show a

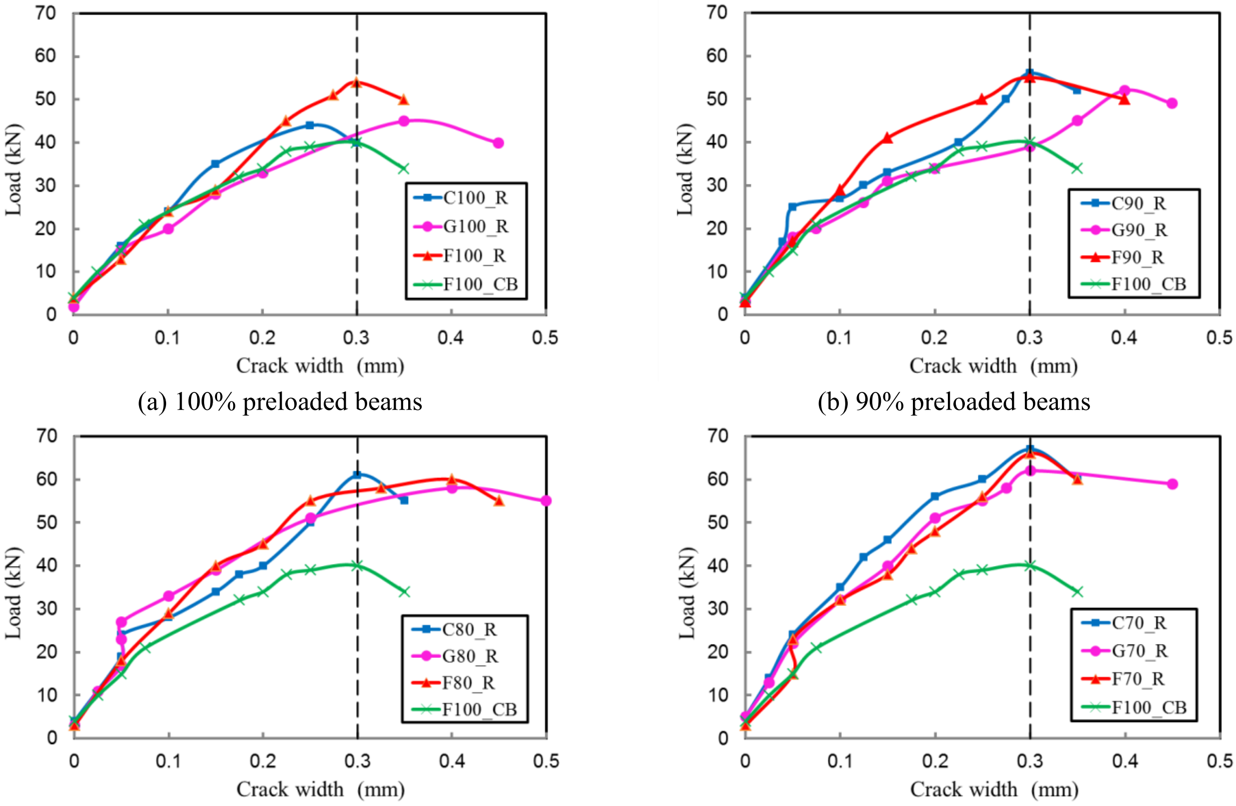

(a) 100% preloaded beams (b) 90% preloaded beams

(c) 80% preloaded beams (d) 70% preloaded beams

Fig. 20 Load-crack width relationships of rehabilitated beams compared at different distress levels

similar pattern with not more than 10% variation in test data. Hence for the comparison purpose, a typical control beam namely, F100_CB was adopted as a reference and is shown in Fig. 20.

It may be noted that, when compared with the control beam, the widths of the cracks were less for the rehabilitated beams at the same level of load irrespective of the composite used for rehabilitation. This verifies the effectiveness of the strengthening procedures adopted. The reduction in crack widths was more at lower levels of pre-distress. Also, it was found that the maximum width of crack did not exceed 0.3 mm which is the serviceability state of crack width as per IS 456 (2000) in the case of (i) all the CFRP rehabilitated and (ii) most of the ferrocement rehabilitated beams at the ultimate stages. However in the case of GFRP specimens at the ultimate level, the maximum crack width has exceeded 0.3mm, but when considering the service load level (ultimate load/load factor; load factor is 1.5 as per IS 456 (2000)), the crack widths were within the limit of 0.3 mm. This confirms the effectiveness of rehabilitation which satisfies the strength and serviceability limit states.

3.5 Cost analysis

The economical aspect of the three selected rehabilitation schemes was compared and presented as a cost analysis in Table 7. The unit price of each scheme was calculated based on the actual prices by considering the number of layers of mats (fibre/wiremesh) used in each scheme. Due to the high price of the carbon fibre mat, the material cost of the CFRP scheme was about ten times that of ferrocement. But the ferrocement scheme is labour intensive and its labour cost was more than FRPs. The soffit area of the beam between the supports, where the laminate was placed was taken to find the total cost per scheme. The cost-efficiency of each specimen was expressed as the ratio of the percentage increase in strength to the total cost.

Table 7 Cost analysis of the rehabilitation schemes

Specimen group no.	Beam mark	% Distress level	Increase in strength (%)	Area (m^2)	Unit price (ξ/m^2) Material	Labour	Total cost (ξ)	Strength to cost ratio (%/ξ)
1 (CFRP rehabilitated)	C100_R	100	13	0.11	2000	675	294	0.04
	C90_R	90	40					0.14
	C80_R	80	53					0.18
	C70_R	70	68					0.23
2 (GFRP rehabilitated)	G100_R	100	13	0.11	1400	975	261	0.05
	G90_R	90	30					0.11
	G80_R	80	45					0.17
	G70_R	70	55					0.21
3 (Ferrocement rehabilitated)	F100_R	100	35	0.11	200	1200	154	0.23
	F90_R	90	38					0.25
	F80_R	80	50					0.32
	F70_R	70	65					0.44

The strength to cost ratio of ferrocement was 1.9, 1.8, 1.8 and 5.8 times than that of CFRP at pre-distress levels

70%, 80%, 90% and 100% respectively. Similarly, it was 2.1, 1.9, 2.3 and 4.6 times than that of GFRP at the above mentioned pre-distress levels. The ferrocement rehabilitation scheme showed better cost-effectiveness over FRP schemes. It was around 1.8 times than CFRP and 2.1 times than GFRP (excluding 100% distress level where the difference is large). When the FRP schemes were compared, the CFRP scheme showed slightly better cost-effectiveness (1.1 times) over GFRP.

5. Conclusions

This study investigated the performance of FRP and ferrocement composites in the flexural rehabilitation of RCC beams. The parameters considered were (i) the strengthening materials and (ii) the pre-distress levels. The following conclusions are arrived at based on the comparative study.

- Rehabilitation of flexural specimens using laminates of CFRP, GFRP, and ferrocement improved the performance of the beams significantly.
- Enhancement of ultimate strength was 35% to 65% for ferrocement rehabilitated beams while that of CFRP was 13% to 68% and GFRP was 13% to 55%. The performance of ferrocement rehabilitated specimens was very close to CFRP and better than GFRP at all the pre-distress levels.
- Ferrocement strengthened schemes maintained similar increases in flexural stiffness (50% to 56%) at all pre-distress levels. Whereas the percentage attainment of stiffness for CFRP was 14% to 49% and that for GFRP was 24% to 34% in the pre-yield stage with the decrease in pre-distress level.
- FRP rehabilitation appeared to have a drastic decrease in energy absorption capacity from 195% to 25% with the increase in pre-distress level, while the ferrocement rehabilitation showed a much lower variation in energy absorption capacity from 205% to 108% with the same increase in pre-distress.
- The energy absorption capacity of ferrocement rehabilitation is higher by an average of 47% than FRP rehabilitation.
- Ferrocement exhibited a better displacement ductility than FRP strengthened beams. This favors the use of ferrocement as a strengthening material over FRP.
- Ferrocement and GFRP showed close values of curvature ductility and were slightly higher than that of CFRP strengthened specimens at lower levels of pre-distress. CFRP appeared to be more brittle when compared to GFRP.
- The crack widths of all rehabilitated beams are within the code specified limits at the serviceable load level, which ensures the serviceability aspect of the strengthening techniques using all these three composites.
- The ferrocement technique is comparable to FRP in all aspects and it can be an economic replacement for the selected FRP composites for rehabilitation purposes.

Acknowledgments

The authors would like to acknowledge the National Institute of Technology Calicut, Kerala, India for extending the facilities for the successful completion of this project.

References

ACI 440.2R (2008), Guide for the Design and Construction of Externally Bonded FRP Systems for Strengthening Concrete Structures, American Concrete Institute, Farmington Hills, MI, USA.

ACI 546R (2014), Guide to Concrete Repair, American Concrete Institute, Farmington Hills, MI, USA.

ACI 549.1R-93 (1999), Guide for the Design, Construction, and Repair of Ferrocement, American Concrete Institute, Farmington Hills, MI, USA.

Al-Kubaisy, M.A. and Jumaat, Z. (2000), "Ferrocement laminate strengthens RC beams", *Concrete Int*., **22**(10), 37-43.

Al-Salloum, Y.A. and Almusallam, T.H. (2003), "Rehabilitation of the infrastructure using composite materials: overview and applications", *J. King Saud Uni.-Eng. Sci*., **16**(1), 1-20. https://doi.org/10.1016/s1018-3639(18)30777-3.

Amran, Y.H.M., Alyousef, R., Rashid, R.S.M., Alabduljabbar, H. and Hung, C.C. (2018), "Properties and applications of FRP in strengthening RC structures: a review", *Struct*., **16**, 208-238. https://doi.org/10.1016/j.istruc.2018.09.008.

Aravind, N., Samanta, A.K., Roy, D.K.S. and Thanikal, J.V. (2013), "Retrofitting of reinforced concrete beams using fibre reinforced polymer (FRP) composites-a review", *J. Urban. Environ. Eng*., **7**(1), 164-175. https://doi.org/10.4090/juee.2013.v7n1.164175.

ASTM D3039/D3039M (2000), Standard Test Method for Tensile Properties of Polymer Matrix Composite Materials, ASTM International, West Conshohocken, PA, USA.

ASTM D7565/D7565M-10 (2017), Standard Test Method for Determining Tensile Properties of Fiber Reinforced Polymer Matrix Composites Used for Strengthening of Civil Structures, ASTM International, West Conshohocken, PA, USA.

Bakis, C.E., Bank, L.C., Brown, V.L., Cosenza, E., Davalos, J.F., Lesko, J.J., Machida, A., Rizkalla, S.H. and Triantafillou, T.C. (2002), "Fiber-reinforced polymer composites for construction-state-of-the-art review", *J. Compos. Constr*., **6**(2), 73-87. https://doi.org/10.1061/(ASCE)1090-0268(2002)6:2(73).

CERA CFR MEMBRANE 230 (2017), Unidirectional Carbon Fibre Reinforcement Membranes for Structural Strengthening; Cera-Chem Private Limited, Chennai, India.

CERA PRIMER EP 18 (2013), High Performance Epoxy Primer for Fiber Wrapping, Cera-Chem Private Limited, Chennai, India.

CERA PRIMER EP S (2013), High Performance Epoxy Saturant for Fiber Wrapping, Cera-Chem Private Limited, Chennai, India.

Ebead, U. (2015), "Inexpensive strengthening technique for partially loaded reinforced concrete beams: experimental study", *J. Mater. Civil Eng*., **27**(10), 04015002. https://doi.org/10.1061/(ASCE)MT.1943-5533.0001249.

Escrig, C., Gil, L. and Bernat-Maso, E. (2017), "Experimental comparison of reinforced concrete beams strengthened against bending with different types of cementitious-matrix composite materials", *Constr. Build. Mater*., **137**, 317-329. https://dx.doi.org/10.1016/j.conbuildmat.2017.01.106.

EW200 (200±20gsm) n.d., E-Glass Fiberglass Cloth/ Fabric/Woven Roving; viewed 06 May 2020, https://chinageomembrane.en.made-in-china.com/product/sXyJhQwrrIYF/China-E-Glass-Fiberglass-Cloth-Fabric-Woven-Roving.html.

Ganesh, P. and Murthy, A.R. (2019), "Repair, retrofitting and rehabilitation techniques for strengthening of reinforced concrete beams - a review", *Adv. Concrete Constr.*, **8**(2), 101-117. https://doi.org/10.12989/acc.2019.8.2.101.

ICRI 310.2R (2013), Selecting and Specifying Concrete Surface Preparation for Sealers, Coatings, and Polymer Overlays, and Concrete Repair, International Concrete Repair Institute, Rosemont, IL, USA.

IS 10262 (2009), Concrete Mix Proportioning-Guidelines, Bureau of Indian Standards, New Delhi, India.

IS 383 (2016), Coarse and Fine Aggregate for Concrete-Specification, Bureau of Indian Standards, New Delhi, India.

IS 456 (2000), Plain and Reinforced Concrete-Code of Practice, Bureau of Indian Standards, New Delhi, India.

Jayasree, S., Ganesan, N. and Abraham, R. (2016), "Effect of ferrocement jacketing on the flexural behaviour of beams with corroded reinforcements", *Constr. Build. Mater.*, **121**, 92-99. https://doi.org/10.1016/j.conbuildmat.2016.05.131.

Kabir, M.I., Subhani, M., Shrestha, R. and Samali, B. (2018), "Experimental and theoretical analysis of severely damaged concrete beams strengthened with CFRP", *Constr. Build. Mater.*, **178**, 161-174. https://doi.org/10.1016/j.conbuildmat.2018.05.038.

Khan, S.U., Rafeeqi, S.F.A. and Ayub, T. (2013), "Strengthening of RC beams in flexure using ferrocement", *Iran. J. Sci. Tech.-Tran. Civil Eng.*, **37**, 353-363.

Kim, Y.J. and Harries, K.A. (2013), "Statistical characterization of reinforced concrete beams strengthened with FRP sheets", *J. Compos. Constr.*, **17**(3), 357-370. https://doi.org/10.1061/(ASCE)CC.1943-5614.0000356.

Masood, A., Arif, M., Akhtar, S. and Haquie, M. (2005), "Rehabilitation of RC and FRC beams by ferrocement- an experimental investigation", *J. Struct. Eng.*, **31**(4), 321-326.

Naaman, A.E. (2012), "Evolution in ferrocement and thin reinforced cementitious composites", *Arab. J. Sci. Eng.*, **37**, 421-441. https://doi.org/10.1007/s13369-012-0187-4.

Naser, M.Z., Hawileh, R.A. and Abdalla. J.A. (2019), "Fiber-reinforced polymer composites in strengthening reinforced concrete structures: a critical review", *Eng. Struct.*, **198**, 109542. https://doi.org/10.1016/j.engstruct.2019.109542.

Nassif, H.H. and Najm, H. (2004), "Experimental and analytical investigation of ferrocement-concrete composite beams", *Cement Concrete Compos.*, **26**(7), 787-796. https://doi.org/10.1016/j.cemconcomp.2003.08.003.

Nayak, A.N., Kumari, A. and Swain, R.B. (2018), "Strengthening of RC beams using externally bonded fibre reinforced polymer composites", *Struct.*, **14**, 137-152. https://doi.org/10.1016/j.istruc.2018.03.004.

Patel, M.R., Tank, T.G., Vasanwala, S.A. and Modhera, C.D. (2015), "Assessment of debonding load for RC beam strengthened with pre-designed CFRP strip mechanism", *Advances in Structural Engineering*, Springer, New Delhi.

Qeshta, I.M.I., Shafigh, P. and Jumaat, M.Z. (2015), "Flexural behaviour of RC beams strengthened with wire mesh-epoxy composite", *Constr. Build. Mater.*, **79**, 104-114. https://dx.doi.org/10.1016/j.conbuildmat.2015.01.013.

Ritchie, P.A., Thomas, D.A., Lu, L. and Connelly, G.M. (1991), "External reinforcement of concrete beams using fibre reinforced plastics", *ACI Struct. J.*, **88**(4), 490-500. https://doi.org/10.14359/2723.

Sarker, P., Begum, M. and Nasrin, S. (2011), "Fibre reinforced polymers for structural retrofitting: a review", *J. Civil Eng. (IEB)*, **39**(1), 49-57.

Saxena, P., Toutanji, H. and Noumowe, A. (2008), "Failure analysis of FRP-strengthened RC beams", *J. Compos. Constr.*, ASCE, **12**(1), 2-14. https://doi.org/10.1061/(ASCE)1090-0268(2008)12:1(2).

Siddika, A., Al-Mamun, M.A., Ferdous, W. and Alyousef, R. (2020), "Performances, challenges and opportunities in strengthening reinforced concrete structures by using FRPs - a state-of-the-art review", *Eng. Fail. Anal.*, **111**, 104480. https://doi.org/10.1016/j.engfailanal.2020.104480.

Sumathi, A. and Arun, V.S. (2017), "Study on behavior of RCC beams with externally bonded FRP members in flexure", *Adv. Concrete Constr.*, **5**(6), 625-638. https://doi.org/10.12989/acc.2017.5.6.625.

Sun, W., Peng, X., Liu, H. and Qi, H. (2017), "Numerical studies on the entire debonding propagation process of FRP strips externally bonded to the concrete substrate", *Constr. Build. Mater.*, **149**, 218-235. https://doi.org/10.1016/j.conbuildmat.2017.05.117.

Tahsiri, H., Sedehi, O., Khaloo, A. and Raisi, E.M. (2015), "Experimental study of RC jacketed and CFRP strengthened RC beams", *Constr. Build. Mater.*, **95**, 476-485. https://doi.org/10.1016/j.conbuildmat.2015.07.161.

Venkateswarlu, C. and Natarajan, C. (2015), "Performance assessment of RC beams with CFRP and GFRP sheets", *Advances in Structural Engineering*, Springer, New Delhi.

Wan, B., Jiang, C. and Wu, Y. (2018), "Effect of defects in externally bonded FRP reinforced concrete", *Constr. Build. Mater.*, **172**, 63-76. https://doi.org/10.1016/j.conbuildmat.2018.03.217.

Wang, X., Zhao, G., Li, K. and Li, M. (2018), "Effect of damage parameter variation on bond characteristics of CFRP-sheets bonded to concrete beams", *Constr. Build. Mater.*, **185**, 184-192. https://doi.org/10.1016/j.conbuildmat.2018.07.031.

CC